Numerical simulation of oscillating-cylinder effects on a downstream cylinder wake using lattice Boltzmann method

Z. Guo[1], Y. Zhou[2*] and C. Zheng[1]
[1] National Laboratory of Coal Combustion, Huazhong University of Science and Technology
Wuhan 430074, P.R. China
[2] Department of Mechanical Engineering, The Hong Kong Polytechnic University
Hung Hom, Kowloon, Hong Kong

ABSTRACT

This paper proposes to use a newly developed lattice Boltzmann technique to simulate the wake of a streamwise oscillating cylinder in the presence of a downstream stationary cylinder. The oscillating frequency ratio f_e/f_s, varies between 0 and 1.8, where f_e is the oscillating frequency of the upstream cylinder and f_s is the natural vortex shedding frequency of an isolated stationary cylinder, and the oscillating amplitude A is fixed at 0.5 cylinder diameter, D. Three typical flow structures, depending on f_e/f_s, have been identified at the cylinder center-to-center spacing L/D = 3.5, which are in excellent agreement with experimental data. The flow structure remains unchanged for the same f_e/f_s as L/D is increased to 6.0, but changes drastically at a low f_e/f_s for L/D = 2.0. It is proposed that, beyond a critical L/D, vortices are formed between the cylinders and the flow structure is independent of L/D. But, below the critical L/D, the free shear layers separated from the upstream cylinder may reattach on the downstream cylinder, thus leading to a different flow structure from that above the critical L/D despite of the same f_e/f_s and A/D. The lift and drag coefficients associated with the two cylinders are examined in detail for each flow structure.

1. INTRODUCTION

Flows around multiple structures are frequently seen in engineering. As the Reynolds number exceeds a critical value, the flow will become unsteady and vortices will shed alternately from the two sides of a structure. The alternate vortex shedding may induce a structural oscillation, which may affect the wake formation and impact upon fluid dynamics around downstream structures. It is of both fundamental and practical importance to study the possible influences of the structural oscillation on the downstream flow. The simplest model for such study is a two-cylinder system, where the two cylinders are either in tandem, side-by-side or staggered arrangements. In the past, most studies focused on the transverse oscillation of one single or two side-by-side cylinders (e.g. Zhou et al. 2001; 2002), perhaps because the lift force is frequently predominant over the drag force. However, the drag force can be important and even exceed the lift, e.g. in the case of a lightly damped structure in a water cross-flow. The experimental or numerical data of the effects of a streamwise oscillation cylinder on a downstream cylinder wake have been scarce.

Xu & Zhou (2002) made perhaps the first attempt to examine such effects experimentally. As the cylinder-oscillating amplitude was fixed at 0.5 cylinder diameter, they have identified three flow regimes as the frequency ratio, f_e/f_s, varied between 0 and 2, where f_e is the oscillating frequency of the upstream cylinder and f_s is the natural vortex shedding frequency of an isolated stationary cylinder. They observed a symmetric binary vortex street for $1.6 \le f_e/f_s \le 2$ and alternative vortex shedding from both cylinders for $0.8 \le f_e/f_s < 1.6$ and $0 < f_e/f_s < 0.8$, though the flow structure corresponding to $f_e/f_s = 0.8 \sim 1.6$ is totally different from that at $f_e/f_s = 0 \sim 0.8$. However, due to the limitation of experiments, many aspects of the physics for this flow remain to be clarified. For example, there was insufficient information on how the oscillating amplitude of the upstream cylinder and the spacing between the cylinders would affect the flow structure; there was no data on pressure field; the dependence on the flow regimes of the drag and lift forces on the cylinders was not measured.

The present work aims to conduct a numerical investigation on this flow using the lattice Boltzmann method (LBM), which is developed in the last few years for computational fluid dynamics (Chen and Doolen 1998), and to complement the experimental investigation by Xu and Zhou (2002).

2. LATTICE BOLTZMANN METHOD

Unlike the conventional direct numerical simulation (DNS) based on the discretization of the Navier-Stokes equations, LBM is based on microscopic model or kinetic equation for a fluid system. Briefly, one considers a fully discrete space-time kinetics of imagined fluid particles moving along a regular lattice and colliding at the lattice nodes, following pre-specified local "collision rules":

$$f_i(\mathbf{x}+\mathbf{e}_i\Delta t, t+\Delta t) - f_i(\mathbf{x},t) = \Omega_i\left(f(\mathbf{x},t)\right), \quad (1)$$

where $f_i(\mathbf{x},t)$ is the distribution function (DF) of fluid particles with a velocity $\mathbf{e}_i$ at position $\boldsymbol{x}$ at time t, and Ω_i is the collision

* Corresponding author. Email: mmyzhou@polyu.edu.hk.

operator, which determines the scatter rate of f_i. One simple collision operator is the so-called BGK operator: $\Omega_i = \tau^{-1}\left(f_i - f_i^{(eq)}\right)$, where τ is the relaxation time and $f_i^{(eq)}$ is the equilibrium distribution function (EDF). The density and velocity of the fluid are defined in terms of the DFs, viz.

$$\rho = \sum_i f_i, \qquad \rho\mathbf{u} = \sum_i \mathbf{e}_i f_i . \tag{2}$$

With an appropriate lattice and EDF, the Navier-Stokes equations and continuity for the incompressible flow can be derived from LBM in the macroscopic time and space scales, viz.

$$\nabla \cdot \mathbf{u} = 0$$
$$\frac{\partial \mathbf{u}}{\partial t} + (\mathbf{u}\cdot\nabla)\mathbf{u} = -\frac{1}{\rho}\nabla p + \nu\nabla^2\mathbf{u} \tag{3}$$

In (3), $p = c_s^2\rho$ is the pressure and $\nu = c_s^2\left(\tau - 0.5\right)\Delta t$ is the shear viscosity, where c_s^2 is a model-dependent parameter.

LBM is characterized by a clear picture of the physics of fluids, the natural parallelism, and ease to handle interactions between fluids or phases (Chen & Doolen 1998). Furthermore, since the pressure is determined from the density through the equation of state for ideal gases at each time step, LBM is much less demanding for computational time, compared with other numerical methods. The reliability and efficiency of LBM have been well demonstrated by a number of studies in various fields. Ladd (1994) managed to apply LBM to a system involving moving bodies in the study of particle suspensions. Aidun et al (1998) and also Qi (1999) improved Ladd's method. The present technique has been developed based on Aidun et al.'s method. However, a new cylinder boundary treatment is presently used in the context of simulating a flow around an oscillating cylinder. Most of previous studies, including Aidun et al.'s method, specified the curved boundary of an object by discrete points at the mid-point between the adjacent nodes of a lattice, which often results in a jagged boundary even for a physically smooth surface. Guo et al. (2002) proposed a boundary treatment for a curved boundary. This treatment applies extrapolation to the non-equilibrium part in DF and preserves the accuracy of the physical boundary without generating a jagged boundary. This treatment is presently used. The second improvement over Aidun et al.'s method is that the object can move fast so that during one time step the object can move a distance larger than one grid spacing. It is well understood that as the object moves in the fluid, a lattice node previously occupied by the object (referred to as *Solid Node, SN*) can become a node occupied by the fluid (referred to as *Fluid Node, FN*) in the next time step and vice versa. One must specify the distribution functions, density, and velocity associated with these new fluid nodes. In Aidun et al's method, the physical variables associated with a new fluid node are approximated by those of its nearest neighboring fluid nodes. However, this approach is only applicable to the case when the object moves slowly so that at least one of its nearest neighbors is a fluid node before and after one time step. For a fast moving object, a cluster of new fluid nodes may be produced, and perhaps some of them are surrounded by new fluid nodes, and the unknown variables cannot be determined by interpolation method. In this case, we directly assign the object velocity to the new fluid nodes, and the DFs are set to be its EDFs with the constant density.

For the purpose of comparison, numerical simulations are carried out in a two-dimensional space at the same conditions as Xu & Zhou (2002)'s experimental data. Two circular cylinders of an identical diameter, D, in a cross flow have a center-to-center spacing of $3.5D$, arranged in tandem. The upstream cylinder oscillates harmonically in the streamwise direction at a fixed amplitude of A/D = 0.5. The Reynolds number, Re, based on D and the free-stream velocity U is 150 ~ 300 (the flow is essentially laminar) and f_e/f_s ranges between 0.5 and 1.8. The computational domain is given by a $40D\times20D$ rectangular area.

3. PRESENTATION OF RESULTS

3.1 *L/D* = 3.5

Figure 1 compares the calculated flow structure with experimental data (Xu & Zhou 2002). The slight difference in Re between numerical calculation and measurement should not invalidate the comparison since A/D and f_e/f_s are the controlling factors of the flow around an oscillating cylinder (Karniadakis & Triantafyllou 1989) and Re is less important. The three flow regimes based on the distinctive flow patterns identified by Xu & Zhou (2002) are reconfirmed numerically. The excellent agreement in the flow structure between the numerical and experimental data provides a validation for the present numerical scheme. In all cases, vortex shedding from the upstream cylinder is locked on with the cylinder oscillation.

At f_e/f_s = 1.8 (two top plates in Figure 1), vortices shed from the upstream cylinder are symmetrically arranged; each structure embraces a pair of counter-rotating vortices (binary vortices). The flow behind the downstream cylinder is characterized by a binary street, consisting of two inner rows of alternately arranged vortices and two outer rows of symmetrically arranged binary vortices. The spatial arrangement of vortices about the centerline results in a lift coefficient, C_L, of no more than 0.2 on either cylinder (Fig 2a). The drag coefficient, C_D, on the downstream cylinder is small but very large on the upstream cylinder (Fig 2b). Correspondingly, the time-averaged lift coefficient, $\overline{C_L}$, and root mean square value, C_L', are small on both cylinders (Table 1). On the other hand, the time-averaged

drag coefficient, $\overline{C}_D$, and root mean square value, C_D', are both very large on the upstream cylinder. Although $\overline{C}_D$ on the downstream cylinder is 0.46, smaller than that (about 1) on an isolated circular cylinder, the corresponding C_D' reaches 0.48, one order of magnitude larger than its counterpart of a single cylinder (e.g. Chen 1987).

As f_e/f_s reduces to 1.08, alternative vortex shedding occurs from both cylinders (middle two plates in Fig 1). The flow structure behind the downstream cylinder is characterized by two rows of vortices: one consists of single vortices, and the other consisting of counter-rotating vortex pairs. This would be clearer if the flow field is extended further downstream (not shown here). The maximum C_L and C_D (Fig 2b) on the downstream cylinder increase significantly, compared with f_e/f_s = 1.8. While the corresponding $\overline{C}_L$ is small, C_L' increases greatly, exceeding that (0.45 ~ 0.75 for Re = 200 ~ 700, Chen 1978) on a single cylinder, as a result from alternating vortex shedding associated with both cylinders. Interestingly, $\overline{C}_D$ as well as C_D' climb considerably.

For f_e/f_s = 0.5, alternative vortex shedding occurs for both cylinders. The successive vortices shed from the upstream cylinders will hit the downstream cylinder alternatively, forming a single staggered street downstream. While the maximum C_D on the downstream cylinder is smaller than that at f_e/f_s = 1.08, the maximum C_L increases marginally. Accordingly, $\overline{C}_D$ and C_D' reduce appreciably, and C_L' increases slightly.

Zdravkovich (1987) classified flows around two tandem stationary cylinders into three flow regimes based on the behaviors of the free shear layers separated from the upstream cylinder. The free shear layers do not reattach on the downstream cylinder and roll up behind it to form the vortex street for $1 < L/D < 1.2 \sim 1.8$, where the upper limit is dependent on Re; they reattach on the upstream side of the downstream cylinder for $1.2 \sim 1.8 < L/D < 3.4 \sim 3.8$. When L/D exceeds 3.4 ~ 3.8, the shear layers roll up alternately, forming vortices between the cylinders, both cylinders generating vortices. Evidently, the flow structures at L/D = 3.5, shown in Figure 1, fall into the third regime, that is, vortices are generated between the cylinders and behind the downstream cylinder, irrespective of the f_e/f_s value.

3.2 *L/D* = 6.0

At L/D = 6.0, the shear layers separated from the upstream cylinder are expected to have sufficient space to form vortices before reaching the downstream cylinder. Therefore, given the same A/D, the flow structures are likely to resemble those at L/D = 3.5. The flow structures (Figure 3) are indeed qualitatively the same as those in Fig 1 for the same f_e/f_s. Nevertheless, there is a slight increase in the maximum spanwise vorticity concentration due to a larger L/D. For example, the maximum $\omega_z D/U$ increases from 1.09 at L/D = 3.5 to 1.15 at L/D = 6 for f_e/f_s = 1.8, from 0.35 at L/D = 3.5 to 0.63 at L/D = 6 for f_e/f_s = 1.08, and from 0.25 at L/D = 3.5 to 0.5 at L/D = 6. The drag and lift coefficients are included in Table 1. Given the same f_e/f_s, C_L' is rather comparable for L/D = 3.5 and 6.0. Compared with L/D = 3.5, $\overline{C}_D$ is slightly larger on both cylinders, but C_D' is appreciably smaller particularly on the downstream cylinder.

3.3 *L/D* = 2.0

At f_e/f_s = 1.8, the shear layers separated from the upstream cylinder manage to form two binary structures, symmetrically arranged about the centerline, before reaching the downstream cylinder. As a result, the flow structure (Fig 4a) at L/D = 2.0 is qualitatively the same as that (Fig 1) at L/D = 3.5. Expectedly, the drag and lift coefficients (Table 1) at L/D = 2 behave quite similarly to those at L/D = 3.5 except C_D' on the downstream cylinder which is larger due to a smaller L/D.

As f_e/f_s reduces to 1.08, the rolling-up shear layers separated from the upstream cylinder reattach on the upstream side of the downstream cylinder before completely forming vortices (Fig 3b). The flow structure between the cylinders is thus not quite the same as that at L/D = 3.5. Nonetheless, the flow structure behind the downstream cylinder is qualitatively the same (c.f. Fig 1). The difference in the vortex formation associated with the upstream cylinder leads to a significant difference in the drag and lift coefficients between L/D = 2.0 and 3.5. C_D' and C_L' at L/D = 2 (Table 1) on both cylinders are almost halved, compared with those at L/D = 3.5. Furthermore, $\overline{C}_D$ at L/D = 2.0 is also reduced, in particular on the downstream cylinder.

A further reduction in f_e/f_s to 0.5 results in a completely different flow structure. The two free shear layers separated from the upstream cylinder (Fig 3c) now roll up symmetrically about the centerline and, before the complete formation of vortices, reattach on the upstream side of the downstream cylinder. As a matter of fact, the free shear layers also tend to separate, symmetrically with respect to the centerline, from the downstream cylinder. Consequently, the flow structure behind the downstream cylinder is rather different from that at L/D = 3.5. Consequently, C_D' and C_L' on both cylinders are drastically reduced, down to about nearly 20% of those at L/D = 3.5. $\overline{C}_D$ on both cylinders also drops substantially; in fact, a negative thrust occurs on the downstream cylinder.

4. CONCLUSIONS

The effects of a streamwise oscillating cylinder on a downstream cylinder wake has been numerically investigated, which leads to

following conclusions.

1. A LBM technique has been developed. One of the major advantages of this technique is ease to handle the moving boundary. The calculated flow is in excellent agreement with measurements, thus providing a validation for the present numerical technique.

2. The numerical investigation reconfirms Xu & Zhou (1992)'s experimental findings of three typical flow structures as f_e/f_s varies between 0 and 1.8 (L/D = 3.5 and A/D = 0.5). Correspondingly, the mean and fluctuating drag and lift coefficients vary significantly for different flow structures.

3. As L/D exceeds 3.5, the flow structures are essentially the same as those at L/D = 3.5 for the same f_e/f_s, which may be identified with one flow regime, which is characterized by the complete formation of vortices between the cylinders. At L/D = 2.0, the flow structure is still similar to that at L/D = 3.5 for f_e/f_s =1.8 since the free shear layers from the upstream cylinder again form vortices before reaching the downstream cylinder. However, as f_e/f_s reduces to 1.08, the free shear layer reattachment on the downstream cylinder occurs, leading to a different flown structure between the cylinders. At f_e/f_s = 0.5, the free shear layers separate symmetrically from both cylinders. As a result, the flow structure is totally different from that at L/D = 3.5 and the mean and fluctuating drag and lift coefficients are also drastically different.

Table 1. Drag and lift coefficients for different f_e/f_s and L/D (A/D = 0.5).

L/D	f_e/f_s	Upstream cylinder				Downstream cylinder			
		$\overline{C}_D$	$\overline{C}_L$	C_D'	C_L'	$\overline{C}_D$	$\overline{C}_L$	C_D'	C_L'
6.0	0.5	1.54	0.000	0.505	0.540	0.988	0.000	0.357	1.02
	1.08	2.084	0.000	1.397	1.602	1.030	0.000	0.292	0.714
	1.8	1.794	0.000	3.449	0.052	0.550	0.000	0.084	0.085
3.5	0.5	1.37	0.00	1.43	0.597	0.77	0.00	0.93	1.003
	1.08	1.99	-0.027	2.41	1.499	1.08	-0.095	1.22	0.961
	1.8	1.62	0.000	3.71	0.084	0.46	0.000	0.48	0.091
2.0	0.5	1.263	0.000	0.541	0.110	-0.166	0.000	0.294	0.116
	1.08	1.676	0.000	1.376	0.820	0.373	0.000	0.736	0.490
	1.8	1.69	0.000	3.50	0.035	0.4667	0.000	0.7692	0.043

ACKNOWLEDGEMENTS

YZ wishes to acknowledge support given to him by the Central Research Grant of The Hong Kong Polytechnic University through Grant G-T408.

REFERENCES

Aidun C.K., Lu Y.N., & Ding E. 1998 Direct analysis of particulate suspensions with inertia using the discrete Boltzmann equation, J. Fluid Mech. 373: 287-311.

Chen S. & Doolen G., 1998 Lattice Boltzmann method for fluid flows, *Ann. Rev. Fluid. Mech,* 30:329.

Chen, S. S. 1978 Flow-induced vibration of circular cylindrical structures (p.260), Hemisphere Publishing Corporation, New York.

Guo Z., Zheng C., & Shi B., 2002 An extrapolation method for boundary conditions in lattice Boltzmann method, *Phys. Fluids,* 16, 2007 (2002).

Karniadakis G. E. & Triantafyllou G., 1989 Frequency selection and asymptotic states in lamina wakes. *J. Fluid. Mech* 199: 441-469.

Ladd A.J.C. 1994 Numerical simulations of particulate suspensions via a discretized Boltzmann equation Part I. Theoretical foundation, *J. Fluid. Mech.* 271:285.

Qi D.W. 1999 Lattice Boltzmann simulations of particles in nonzero Reynolds number flows, *J. Fluid Mech,* 385:41-62.

Xu, S. J. and Zhou, Y. 2002 Effect of a streamwise oscillating cylinder on a downstream cylinder wake, *Proceedings of 11th international Symposium on Applications of Laser Techniques to Fluid Mechanics* (CD Rom), Lisbon, 8-11 July, 2002. Paper 34.4.

Zdravkovich, M.M. 1987. The effects of interference between circular cylinders in cross flow. *ASME Journal of Fluids Engineering*, **1**, 239-261.

Zhou, Y., Wang, Z. J., So, R. M. C., Xu, S.J. and Jin, W. 2001 Free vibrations of two side-by-side cylinders in a cross flow, *Journal of Fluid Mechanics*, **443**, 197-229.

Zhou, Y., Zhang, H. J. & Yiu, M.W.: 2002 The Turbulent Wake of Two Side-by-Side Circular Cylinders, *J. Fluid Mech.* **458**, 303-332.

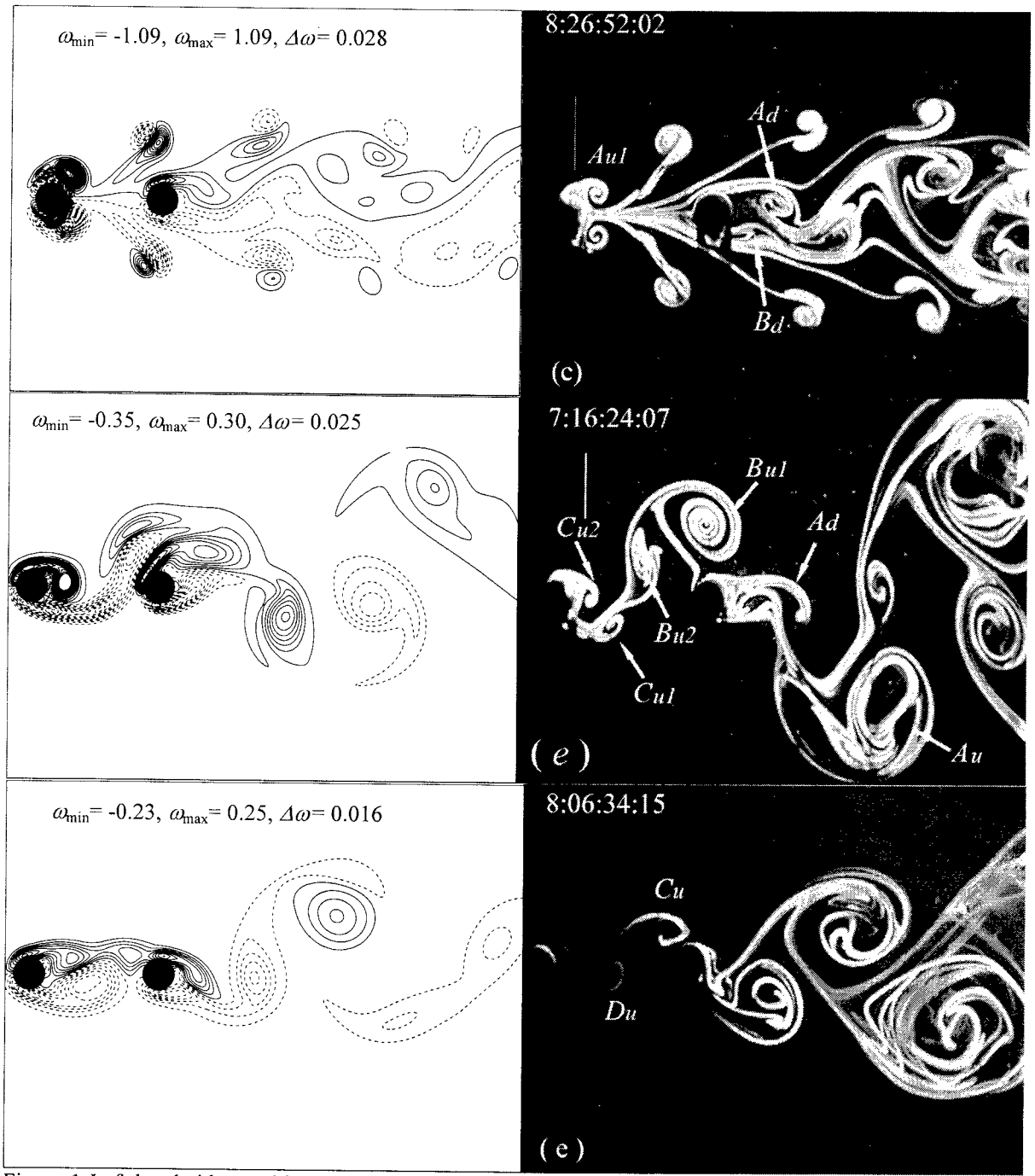

Figure 1 Left-hand side: positive (dashed line) and negative (solid line) vorticity contours from numerical simulation (Re=150); right-hand side: streaklines from Xu & Zhou (2002)'s flow visualization in a water tunnel using the LIF technique. A/D = 0.5, L/D =3.5; f_e/f_s =1.8 (Re = 300), 1.08 (300), and 0.5 (150) from top to bottom.

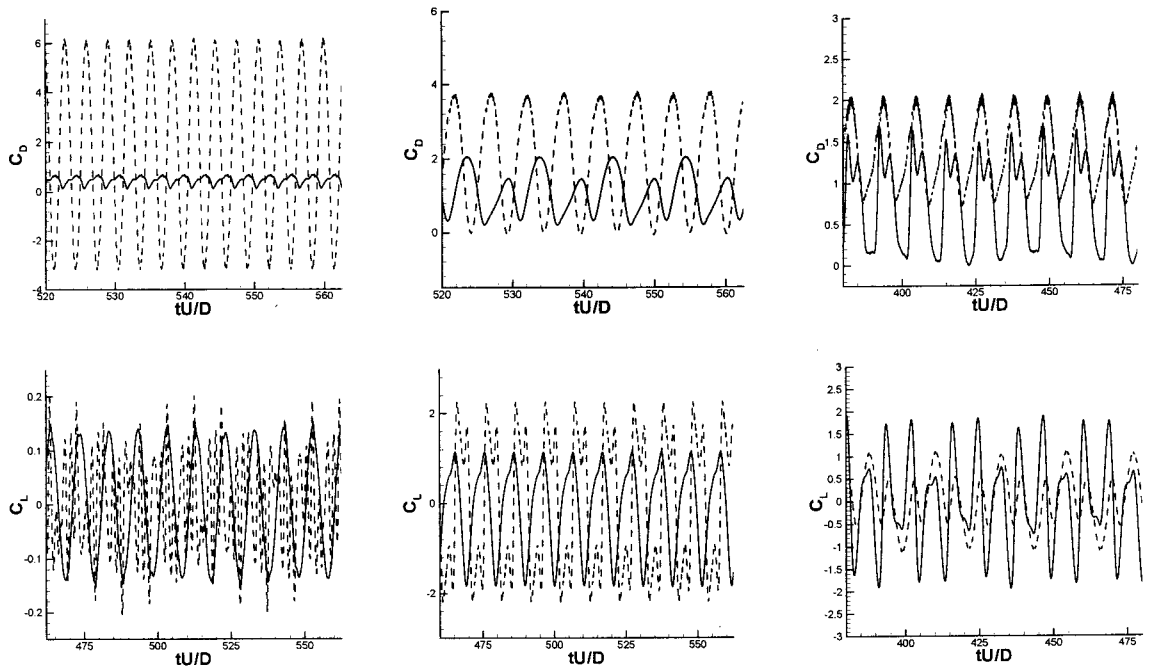

Figure 2 Time histories of the drag and lift coefficients of the upstream and downstream cylinder with A/D = 0.5, L/D = 3.5. (a) f_e/f_s = 1.8, (b) 1.08, (c) 0.5. Dashed line: upstream cylinder; Solid line: downstream cylinder.

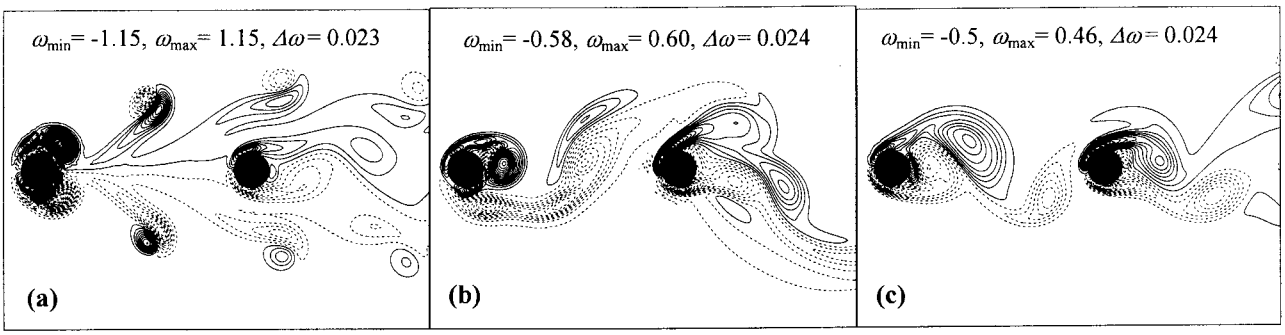

Figure 2 Time histories of the drag and lift coefficients of the upstream and downstream cylinder with A/D = 0.5, L/D = 3.5. (a) f_e/f_s = 1.8, (b) 1.08, (c) 0.5. Dashed line: upstream cylinder; Solid line: downstream cylinder.

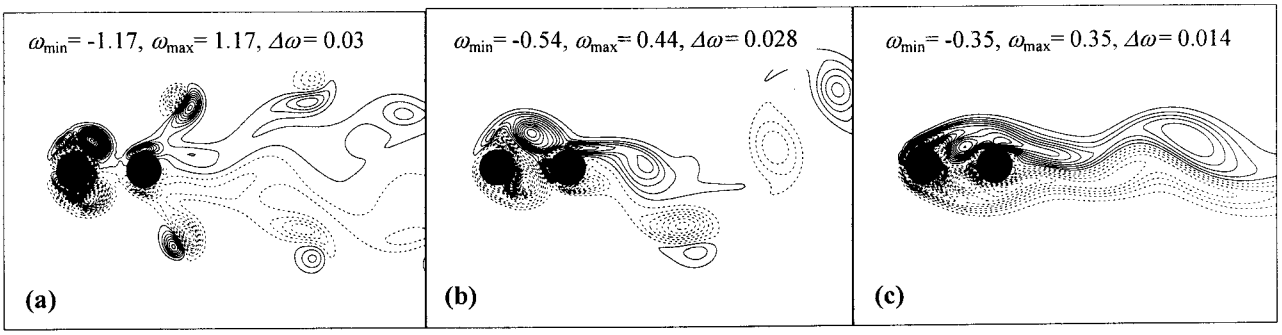

Figure 4 Positive (dashed line) and negative (solid line) vorticity contours from numerical simulation: (a) f_e/f_s = 1.8; (b) 1.08; (c) 0.5. A/D = 0.5, Re=150, L/D =2.